SIMILARITIES AND GEOMETRICAL EFFECTS ON ROTATING CAVITATION IN TWO SCALED CENTRIFUGAL PUMPS

Michael HOFMANN, Bernd STOFFEL
Laboratory for Turbomachinery and Fluid Power (TFA),
Darmstadt University of Technology
Magdalenenstrasse 4, 64289 Darmstadt, Germany
Tel.: +49-6151-16-2153
stoffel@tfa.tu-darmstadt.de

Jens FRIEDRICHS, Günter KOSYNA
Pfleiderer-Institut für Strömungsmaschinen (PFI),
Technical University of Braunschweig
Langer Kamp 6, 38106 Braunschweig, Germany
Tel: +49-531-391-2928
j.friedrichs@tu-bs.de

ABSTRACT

Two scaled centrifugal pumps with vaneless radial diffuser running at identical Reynolds-Numbers are in the focus of experiments at Technical University of Braunschweig and Darmstadt University of Technology in the frame of a cooperation hosted by the DFG (Deutsche Forschungsgemeinschaft). Both pumps can hold different runner geometries as well as different leading edge geometries within the same runner. This paper describes experimental investigations of different configurations in both pumps. All configurations show the occurrence of a periodic cavitation state called “rotating cavitation” in a wide range of part load conditions, which onset can be characterized by an almost constant value of the dimensionless parameter $\sigma/2\alpha$. Comparison of the main characteristics of both pumps as well as optical investigations to determine the dynamic properties in cavitating conditions have been carried out.

1. NOMENCLATURE

b	passage width	
d	diameter	
f	frequency	
g	gravity	
H	head	
M	mass-flow-gain factor	
n	impeller rotating speed	
n_s	specific speed	$333*n*\dot{V}^{1/2}/(g*H)^{3/4}$
p	static pressure	
p_v	vapor pressure	
U	upstream mean velocity	
$\dot{V}$	volume flow	
z	number of blades	
α	incidence angle	
β	blade angle	
ρ	density	
η	efficiency	
σ	cavitation number	$2*(p_1-p_v)/\rho U^2$
φ	flow coefficient	$4*\dot{V}/(d_2^3\pi^2 n)$
ψ	pressure rise coefficient	$2*gH/(d_2^2\pi^2 n^2)$
1	inlet	
2	outlet	
D	design point	
IC	incipient cavitation	

2. INTRODUCTION

Cavitation and its related effects are still playing a major role in design and use of centrifugal pumps. In order to improve the understanding of the interaction between the cavitation phenomenon and its erosive impact on one hand and the effects on pump head-drop on the other hand a cooperation between the Laboratory for Turbomachinery and Fluid Power (TFA) and the Pfleiderer-Institute (PFI) has been carried out sponsored by the Deutsche Forschungsgemeinschaft (DFG). The first aim of the project was to ensure a entire similarity of both pumps in all operating points and states of cavitation as a major requirement for all the following investigations. In order to prove this similarity not only the pump characteristic but especially the shape of the head-drop curves was compared using

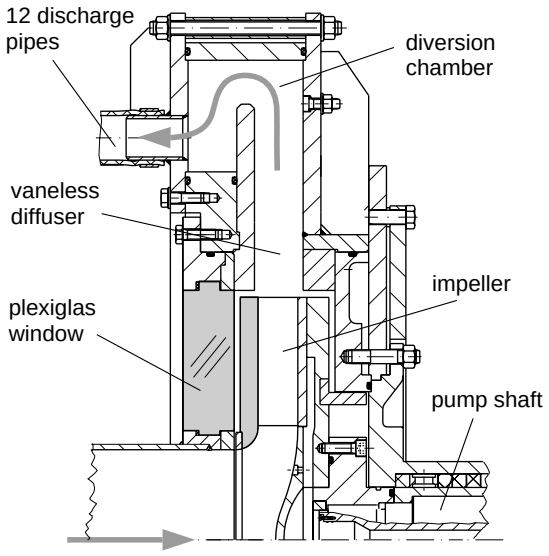

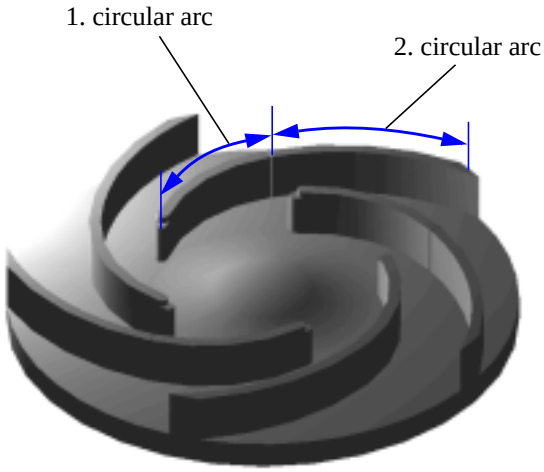

Figure 1: a) Cross-sectional view of the test-pump **b) 3D-view on 2-circular-arc impeller**

the dimensionless coefficients ψ, φ, and σ. A new effect of particular interest influencing the head-drop in a significant way is the so-called “rotating cavitation”, which was observed in both pumps. This type of cavitation is characterized by a “creeping head-drop”, a very soon beginning of decreasing pump delivery head, and it therefore has a strong influence on the $NPSH_{3\%}$-figures [10], [3], [4].

Most of the information about rotating or alternating cavitation in the available literature is concerned with this phenomenon occurring in inducers of rocket-turbopumps. In 1997 Tsujimoto et al. [11] observed several different modes of rotating cavitation in the H-II turbopump-inducer, while De Bernardi and Jousselin [2] investigated cavitation instabilities of the ARIANE-V turbopump. Theoretical analyses were performed by Tsujimoto et al. [12] and Greitzer [6].

In another theoretical stability analysis for a cascade, Watanabe et al. [13] demonstrated in 1999 that rotating cavitation basically depends on the ratio of cavitation number to twice the incidence angle ($\sigma/2\alpha$). Huang et al. [9] presented in 1998 an experimental investigation of an inducer with alternating cavitation, including typical head-drop curves. In 2000 Horiguchi et al. [8] investigated in another cascade analysis the influence of the cascade parameters (solidity and stagger angle) on the onset and development of rotating cavitation. The authors also explained the mechanism of the phenomenon to be caused by an interaction of the local flow near the cavity closure region and the leading edge of the following blades.

3. EXPERIMENTAL SETUP

At the PFI the effect of rotating cavitation was observed in two similar single-stage centrifugal pump impellers [3], a 1-circular-arc impeller (not described in this paper) and a 2-circular-arc impeller. At TFA the rotating state of cavitation was found in the scaled 2-circular-arc impellers with 3 different leading edge geometries, comparable to the geometries tested in [1] and [7], with one skewed and 2 non-skewed edges. The model pump at TFA has a scale factor $\mu_g = 0.5$ which is applied to all parts of the whole pump and is therefore running with a rotational speed $n_{TFA} = 4*n_{PFI}$ to obtain the same Reynolds number. This scaling was chosen to obtain a higher velocity ratio and consequently a higher rate of erosive impact which is the main aim of investigations at TFA.

All impellers were tested in a closed-circuit system with variable system pressure. In order to generate a uniform circumferential pressure distribution at the impeller outlet, a vaneless radial diffuser was used instead of a volute. The diffuser itself was connected to the upstream system by twelve discharge pipes. Figure 1a shows a cross-sectional view of the pump. The impeller shroud and also the shroud-sided casing are made of plexiglas to enable direct observations of the impeller. The impeller blades consist of two circular arcs, a smaller one from inlet to nearly half of the chord and a larger one up to the outlet. This simple impeller-geometry was chosen to obtain at least approximately a 2D flow field on one hand and to ensure a good accessibility for the measurement technique on the other hand, see fig. 1b. In Table 1 the design parameters of both impellers are presented.

Optical measurements

To perform visual analysis of rotating cavitation a digital video camera operating in frame integrating mode was used at PFI and a 12-bit CCD-camera at TFA, both together with a frame-grabber device and a stroboscopic light source. At the TFA also a Laser-Light-Sheet-Technique was used for illumination of the optical observations. Due to the limited sampling rate, an additional high speed camera with a sampling rate up to 40,000 frames per second was used at both institutes to record sequences of rotating cavitation. These sequences allowed us to analyze the development of single unsteady cavities during one or more revolutions.

Impeller		PFI	TFA
Blade shape		2-circular-arc	2-circular-arc
Scale factor	μ	1.0	0.5
Inlet-$\varnothing$	d_1	260mm	130mm
Outlet-$\varnothing$	d_2	556mm	278mm
Blade inlet angle	β_1	19^o	19^o
Blade outlet angle	β_2	23^o	23^o
Passage width	b	46mm	23mm
Number of blades	z	5	5
Specific speed	n_s	27.5	27.5
Blade thickness	s	13mm	6.5mm
Rotating speed	n	9Hz	36Hz

Table 1: Design parameters of both impellers

4. RESULTS AND DISCUSSION

Overall performance and head-drop-curves

In fig.2a the performance of both pumps is shown, described by pressure rise coefficient ψ and flow coefficient φ. Although there is a small difference in the absolute performance the match of both curves is pretty good. Especially the gradient in pressure rise and the slight discontinuity between a flow coefficient of 0.025 and 0.03 shows a very similar behavior. In addition fig. 2b contains the cavitation number of incipient cavitation (σ_{IC}) for both pumps, derived from optical observations of the very beginning cavitation. In both cases the design point of φ_D=0.03 (420m^3/h and 210m^3/h respectively) matches the σ_{IC}-curve, showing the expected minimum at this point. At flow coefficients lower than design point, incipient cavitation occurs on suction side, above the design point on pressure side of the blade. At the design point cavitation starts nearly simultaneously on both sides of the blade.

In fig. 3 the head-drop-curves of both pumps are presented for different relative flow rates. The curves of 1.00 and 0.80 are directly comparable between TFA and PFI. They are showing an almost identical shape in both pumps. The curve of relative flow rate 1.00 is characterized by a very constant pump head over a wide range and a slight head rise just before the typical “sudden head-drop”; while the relative flow rate of 80% shows a sooner and more uniform head rise followed by a weaker head-drop which can still be described as “sudden head-drop”.

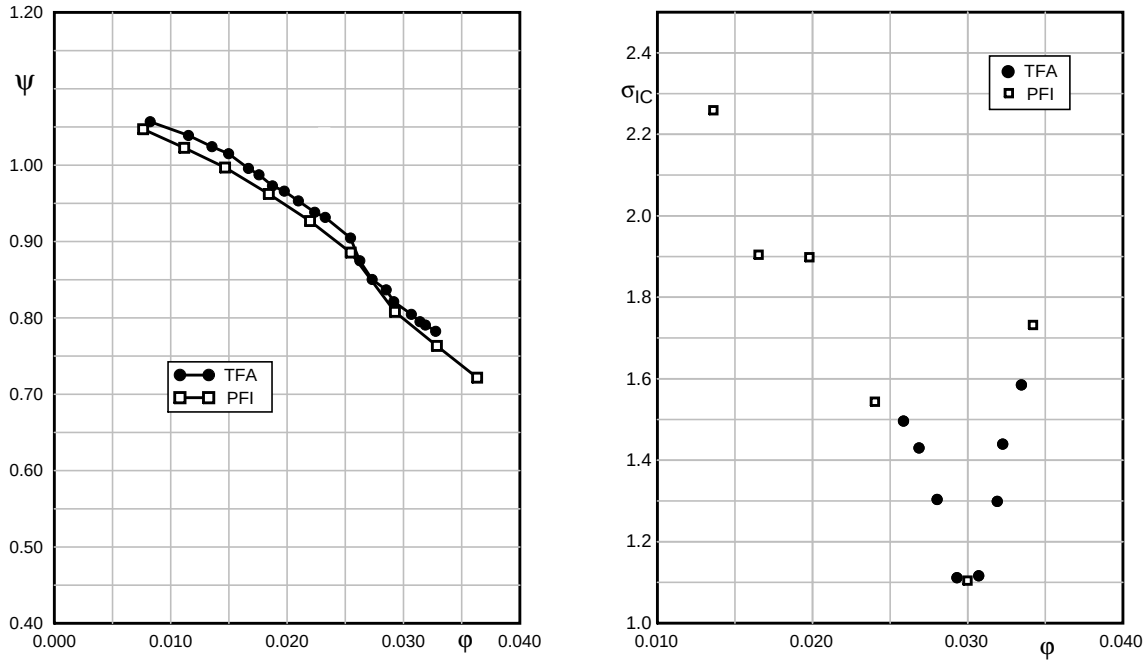

Figure 2: a) Impeller performance characteristic and b) incipient cavitation

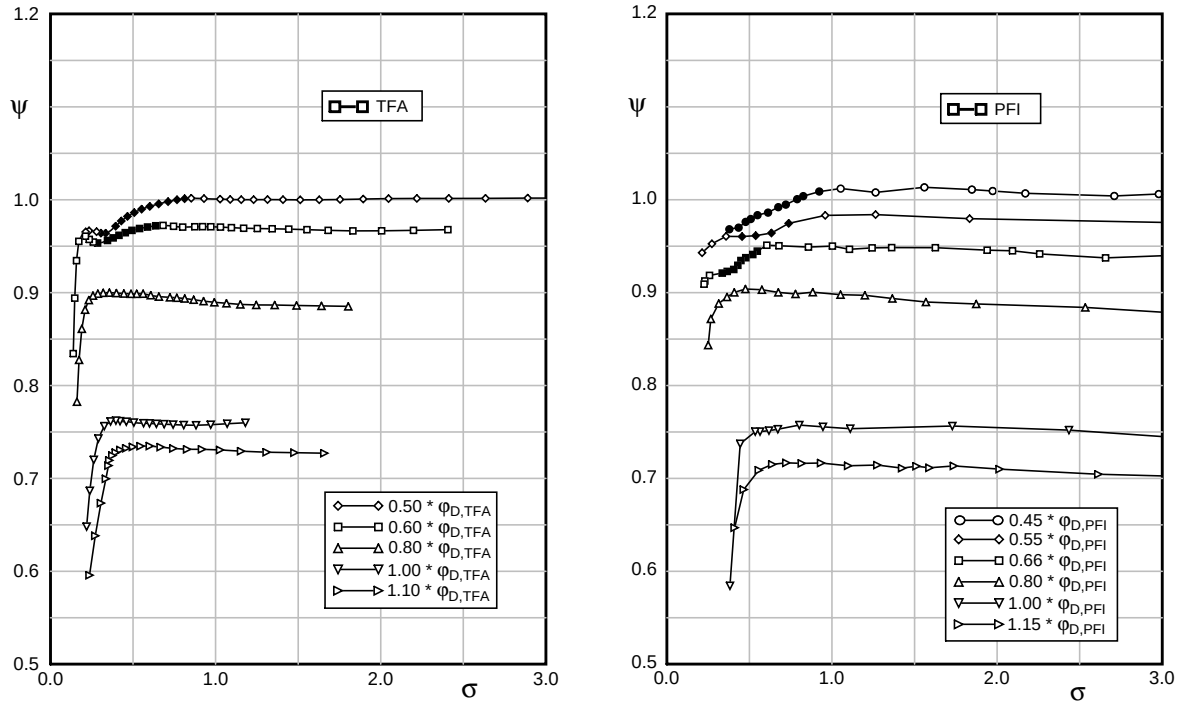

Figure 3: Head-drop-curves at different flow coefficients TFA (left) and PFI (right).

The other curves have different relative flow rates but the differences are still small so that their shape can also be compared. The flow rate of 1.10 again shows a slight and uniform head rise followed by a "sudden head-drop". The remaining part load curves are of special interest: All of them show the "creeping head-drop" and the cavitation number of the beginning head-drop increases for decreasing flow rates. At lower cavitation numbers a slight recover in pump head like a saddle can be found in both pumps at relative flow rates between 66% and 50% just before the final head-drop occurs.

In summary the pump-performance and the head-drop curves in both pumps show a very good agreement. In combination with the σ_{IC}-characteristic, the similarity of the two pumps is proved.

Rotating cavitation

The state of rotating cavitation was observed in both pumps using a stroboscopic light source. In this observation the phenomenon appears as a significant fluctuation in the cavity length assigned to each blade. Considering the neighboring blades a phase lag between the fluctuation cycles of each blade can be found.

Rotating cavitation is indicated by filled symbols in the head-drop-curves of 66% part load and lower flow rates in fig. 3. Those parts of the curves which are assigned to rotating cavitation show the described significant creeping head-drop, beginning just at the point where rotating cavitation occurs. A remarkable fact is, that the phenomenon disappears in both pumps in the curves between 66% and 50% at lower cavitation numbers (σ=0.3...0.4). The pressure rise coefficient recovers slightly just after rotating cavitation has disappeared followed by a more sudden head-drop, when the cavitation number decreases further. At relative flow rates lower than 50% the creeping head-drop also starts in combination with the occurrence of rotating cavitation but this time the phenomenon remains unto the end of the head-drop curve (a head-drop of more than 3%).

The observed behavior of creeping head-drop is well known, mostly for impellers of medium or higher specific speed; although normally no rotating cavitation was reported for those machines. Huang et al. [9] presented head-drop-curves of an inducer showing a very similar behavior of creeping head-drop for operating points with occurrence of cavitation oscillation.

Another important result of fig. 3 is the position of onset of rotating cavitation. Decreasing the flow rate, the cavitation number of beginning rotating cavitation ($\sigma_{I,Rot}$) increases. In fig. 4 the parameter $\sigma/2\alpha$ for onset of rotating cavitation is shown. The incidence angle α was calculated using a constant meridional velocity without swirl as inlet condition.

The parameter σ/2α for the beginning of rotating cavitation is within a small band of σ/2α = 2.3 +/-0.2. Especially in the results of the PFI-pump, which can easier be observed for rotating cavitation due to the size and lower speed, the parameter is nearly constant for all flow rates and both leading edge geometries.

With this result, the phenomenon can be understood as an impeller stability problem, which is driven by the increasing cavity volume (or cavity length) in relation to the incidence angle, according to [12] and [6]. Due to the developed state of the cavity at this operating points (see fig. 6) the leading edge geometry is less relevant for the beginning of rotating cavitation (but it has a strong influence onto σ_{IC}).

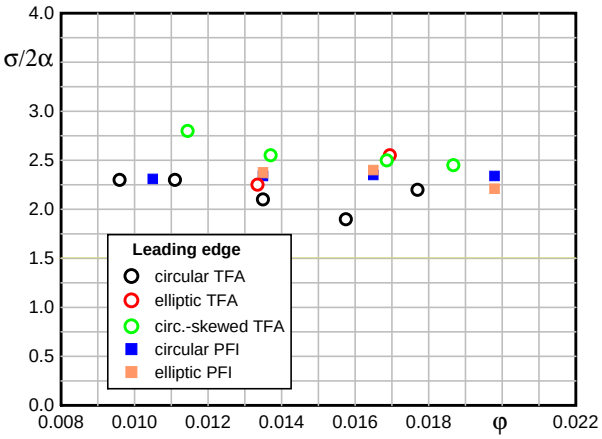

Figure 4: Onset of rotating cavitation for different leading edge geometries

Figure 5 shows a highspeed sequence recorded with 2000 fps at the TFA impeller with inverted colors. Between each frame the impeller rotates approximately 6.5° in anticlockwise direction. From 0° to 19.5° the cavity on the suction side of first blade can be seen moving with the blade. In addition on the pressure side of the following blade a small cavity can be found just across from the ending region of the main suction side cavity. Between 26.0° and 39.0° the larger cavity is partially covered by a casing strut, while the following blade moves into the windows. This following blade shows no suction side cavitation.

From a similar highspeed investigation of the impeller during several revolutions at PFI it can be found that there are two “cells” of fully developed suction side cavitation within the impeller separated by passages with a very small or without cavity. In fig. 6 a sequence of sketches derived from highspeed-film is presented for a flow rate φ=0.0165. These sketches are real time-resolving showing the same blades at a fixed angular position after each revolution. At the first revolution blade 1 shows a separated cloud cavitation and the following blade 2 a very small attached cavity. One revolution later the cavity of blade 1 is large but attached, while at blade 2 strong cloud cavitation occurs.

The next two revolutions (3 and 4) the cavity of blade 1 shrinks and at revolution 5 and 6 the blade shows a small cavity, while the cloud cavitation of blade 2 has developed into an attached cavity. In the following this cavity becomes still smaller (rev. 7 and 8) and a new cloud cavitation develops at blade 1. At revolution 9 a state somewhere between rev. 1 and 2 is reached again.

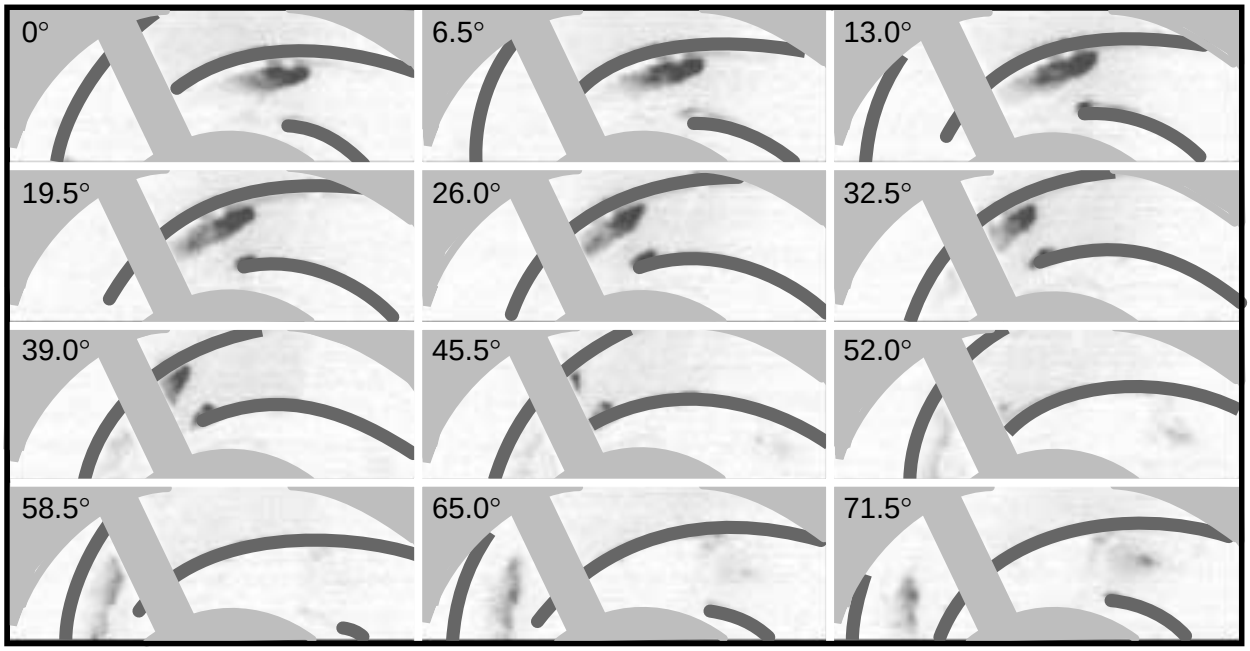

Figure 5: Two following passages under rotating cavitation (φ=0.0136, σ=0.55)

The phenomenon of rotating cavitation is therefore based on an interaction of two (or more) adjacent passages; a decreasing cavity moving with a blade is combined with an increasing cavity at the following blade. In the impeller relative-system the cavitation seems to move in clockwise direction.
To explain the interaction between adjacent blades in fig. 7 snapshots of rotating cavitation are shown. The order of the frames is not a time-resolving sequence thus the frames allow only to analyze different states of one blade in rotating cavitation but not their time-dependent development. The upper row (a) shows three different snapshots of cavitation-states occurring during rotating cavitation. In the lower row (b) each state is shown again, this time represented by a blade fitted with an array of fiber-probes (3 probes along blade width) to indicate the local flow direction. Due to their negligible inertia and the low significant frequencies of rotating cavitation, the probes can be used to obtain information about the flow direction even in unsteady states. Figure 8 shows the quasi-steady state before rotating cavitation occurs. Because of a slightly different angle of view and of light, the cavity in the lower row seems less bright compared to the upper row of fig. 7.
Frame 1a and b show a state characterized by a separated cavity of extreme thickness and length. The suction-side probes also indicate the separation of the cavity. In comparison, the pressure-side probes are orientated at a small angle to the blade, in 1b even smaller than in the reference fig. 8. In frame 2a and b the cavity is small and thin; the suction-side probes are attached to the blade while the pressure-side probes are clearly separated. A similar small cavity can be seen in frame 3a and b but this time the probes indicate even severe backflow in the pressure-side passage.

From analysis of fig. 5 to 7 two different significant states of rotating cavitation can be described:

i. A small and very thin cavity on suction side is observed together with a large cavity of the blade ahead, which reaches into the passage. In this passage the flow is dominated by backward orientated components.

ii. A large cavity on suction side according to an increased local incidence angle means forward flow in the pressure-side passage, probably even with a higher flow rate compared to steady state

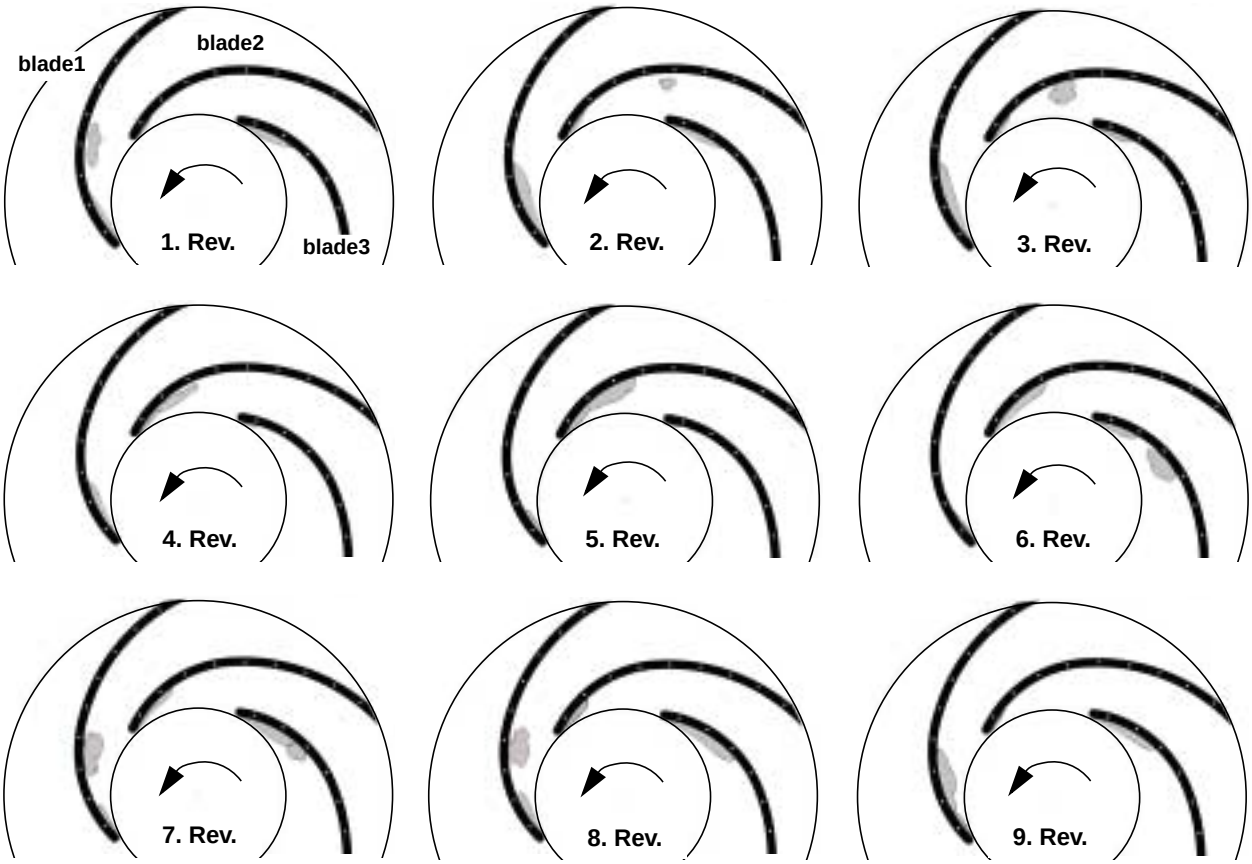

Figure 6: Sketches of rotating cavitation from high-speed-film (φ=0.0165, σ=0.6)

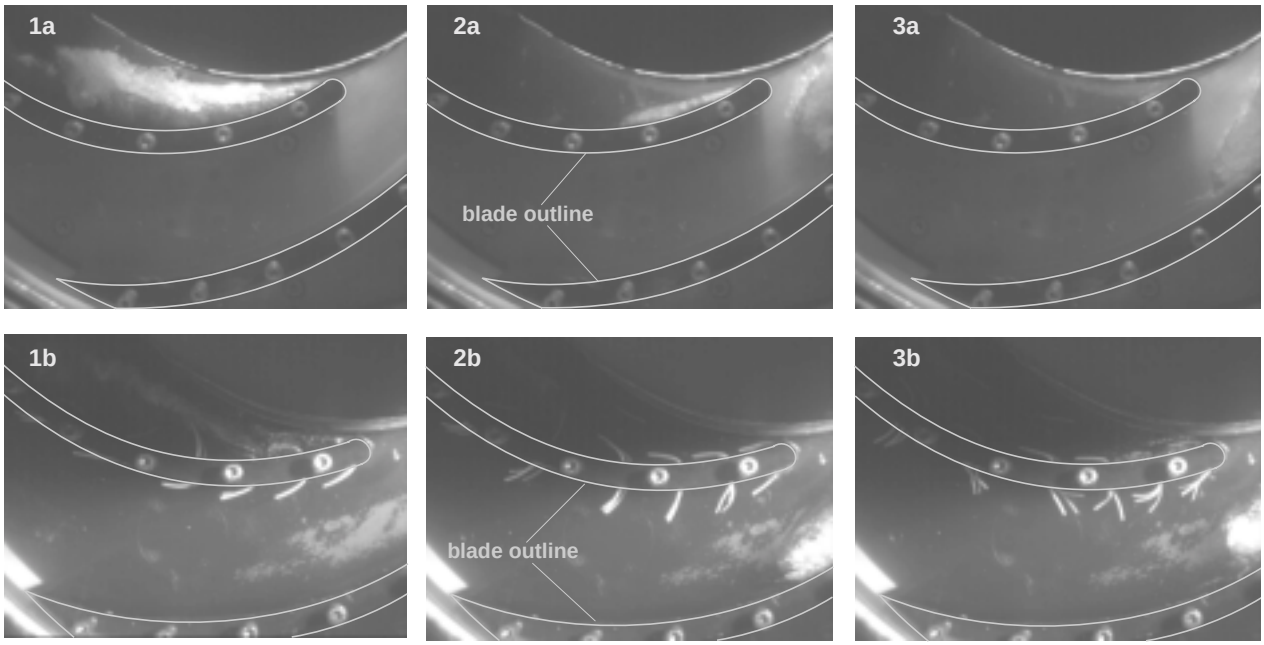

Figure 7: Snapshots of rotating cavitation at 45% part load (φ=0.0136), fiber probe fitted blade (bottom row)

According to the analysis of Horiguchi et al. [8] and with respect to fig. 5 to 7 the mechanism can be explained as follows: A large separated cavity (with cloud cavitation) means blockage for the suction-side passage. Therefore the flow rate in the following passage increases leading to a decrease in the local incidence angle. In addition, the closure region of the larger cavity of the first blade generates a velocity component with direction onto the blade surface which also decreases the incidence angle of the following blade. Thus the following blade shows a very small cavity. If the cavity of the first blade becomes smaller, both effects, namely the blockage and the induced velocity, decrease, leading to a rapid increase in the incidence angle of the following blade.
The interaction of the cavity of the first blade and the following blade becomes even stronger if either the cavity becomes larger or the separation angle between cavity and blade increases, both effects are leading to a cavity closer toward the pressure side of the following blade. This observation matches fig. 4 meaning that for an increased incidence angle α of the steady flow the cavitation number σ can be higher for the same risk of rotating cavitation.

In developed rotating cavitation two adjacent passages are operating at different points of the impeller characteristic. The blocked passage at a point with a lower flow coefficient and the following, unblocked passage at a higher flow coefficient compared to the mean flow coefficient of the current pump operating point [9]. Consequently the lower flow coefficient means a stronger pressure rise in the passage and the higher flow coefficient means a weaker pressure rise based on the current pump pressure rise (see fig. 2a). The stronger pressure gradient suppresses the development of cloud cavitation further into the passage while the depression of the static pressure rise in the next passage allows the clouds to be carried forward in it.

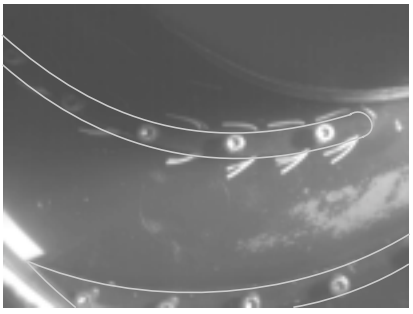

Figure 8: Quasi-steady state at 45% part load

Considering the whole impeller the pump performance is a mean value of each passage pressure rise and flow. In increasing rotating cavitation and therefore increasing cavity size the blocked passage can not completely adopt the missing pressure rise of the passages with higher flow particularly with regard to the increasing backflow components. In sum the pump head decreases gradually (“creeping head-drop”) in rotating cavitation.

Further analysis of the typical frequencies of the phenomenon by unsteady pressure measurement in both pumps (not described in this paper) and optical observation showed that the rotating speed of the cavitation is lower than the impeller speed (about 30%-60%) and it is rotating in clockwise direction in a impeller-relative system [5], [7].

5. CONCLUSIONS

1. Two scaled pumps of low specific speed were investigated running at the same Reynolds number. The agreement in performance and particularly in the shape of head-drop is very good and proves the similarity of the pumps.
2. Rotating cavitation was observed in both pumps at relative flow rates below 70%. The phenomenon is assigned to a typical “creeping head-drop”.
3. The onset of rotating cavitation can be described by the parameter $\sigma/2\alpha$, which is constant for both pumps and all operating points and also independent from the leading edge geometry.
   That means, at operating points of higher incidence angle (part load conditions) the cavitation number can also be higher and thus the state of cavitation can be weaker to produce the same instability.
4. The propagation of the phenomenon can be explained by an interaction of the cavity (related blockage and velocity component near the cavity closure region) and the leading edge of the following blade. Within one impeller-revolution two cells of rotating cavitation were observed at all operating points, rotating relatively against the impeller.

ACKNOWLEDGMENTS

The presented study was carried out in cooperation with DFG (Deutsche Forschungsgemeinschaft).

REFERENCES

[1] Böhm, R., Hofmann, M., Ludwig, G., Stoffel, B., 1998, “Investigations on Possibilities to Control the Erosive Cavitation Aggressiveness by Hydrodynamic Effects”, *Proceedings of the 3rd Int. Symposium on Cavitation, Grenoble, Vol 2*, pp. 121-128.

[2] De Bernardi, J., Jousselin, F., 1993, “Experimental Analysis of instabilities related to cavitation in a turbopump inducer”, *1st International Symposium on Pump Noise and Vibrations.*

[3] Dreiß, A., 1997, “Untersuchung der Laufradkavitation einer radialen Kreiselpumpe durch instationäre Druckmessungen im rotierenden System”, *Diss. TU Braunschweig, publ. in Mitteilungen des Pfleiderer-Instituts für Strömungsmaschinen, Heft 4*, W.H. Faragallah.

[4] Dreiß, A., Kosyna, G., 1997, “Experimental Investigations of Cavitation-States in a Radial Pump Impeller”, *Proceedings of the JSME Centennial Grand Congress, International Conference on Fluid Engineering.*

[5] Friedrichs, J., Kosyna, G., 2001, “Rotating Cavitation in a Centrifugal Pump Impeller of Low Specific Speed”, *Proceedings of ASME FEDSM2001-18084.*

[6] Greitzer, E.M., 1981, “The Stability of Pumping Systems”, *ASME Journal of Fluids Engineering, Vol. 103,* pp. 193-242.

[7] Hofmann, M., “Ein Beitrag zur Reduzierung der erosiven Aggressivität kavitierender Strömungen”, *Diss. TU Darmstadt, to be submitted June 2001*

[8] Horiguchi, H., Watanabe, S., Tsujimoto, Y., Aoki, M., 2000, “A Theoretical Analysis of Alternate Blade Cavitation in Inducers”, *ASME Journal of Fluids Engineering, Vol. 122*, pp. 156-163.

[9] Huang, J.-D., Aoki, M., Zhang, J.-T., 1998, “Alternate Blade Cavitation on Inducer”, *JSME International Journal, Series B, Vol. 41,* pp. 1-6.

[10] Spohnholtz, H.H., 1997, “NPSH-Verhalten von Halbaxialpumpen”, *Diss. TU Braunschweig, publ. in Mitteilungen des Pfleiderer-Instituts für Strömungsmaschinen, Heft 4*, W.H. Faragallah.

[11] Tsujimoto, Y., Yoshida, Y., Maekawa, Y., Watanabe, S., Hashimoto, T., 1997, “Observations of Oscillating Cavitation of an Inducer”, *ASME Journal of Fluids Engineering, Vol. 119*, pp. 775-781.

[12] Tsujimoto, Y., Kamijo, K., Yoshida, Y., 1993, “A Theoretical Analysis of Rotating Cavitation in Inducers”, *ASME Journal of Fluids Engineering, Vol. 115*, pp. 135-141.

[13] Watanabe, S., Sato, K., Tsujimoto, Y., Kamijo, K., 1999, “Analysis of Rotating Cavitation in a Finite Pitch Cascade Using a Closed Cavity Model and a Singularity Method”, *ASME Journal of Fluids Engineering, Vol. 121*, pp. 834-840.